*M&C 2023 - The International Conference on Mathematics and Computational Methods Applied to Nuclear Science and Engineering · Niagara Falls, Ontario, Canada · August 13 – 17, 2023*

# A Digital Twin for Refueling Strategy Simulation of Stable Salt Fast Reactors

**P. Deng[1], W. S. Yang[1], Y. Cao[2], T. Hua[2], L. Godfrey[3], A. Ballard[3a]**

[1]University of Michigan
2355 Bonisteel Blvd, Ann Arbor, Michigan, USA

[2]Argonne National Laboratory
9700 South Cass Avenue, Lemont, Illinois, USA

[3]Moltex Energy
71 Prince William Street, Unit 102, Saint John, New Brunswick, E2L 2B2, Canada

puran@umich.edu, wonyang@umich.edu, ycao@anl.gov, hua@anl.gov,
lukegodfrey@moltexenergy.com, andrewballard@moltexenergy.com

## ABSTRACT

For the development of online refueling strategy for a family of stable salt fast reactors, a digital twin system was developed by wrapping over the legacy fast reactor analysis codes REBUS, DIF3D, and PERSENT. User selections of the constraints on various state parameters such as maximum peak power, maximum reactivity worth of reloaded assemblies, and minimum cycle length are supported to ensure safe operating conditions during refueling. Currently, a refueling assembly position is determined to achieve a user-specified primary objective. To reduce the required user's efforts to investigate refueling strategies, additional flexibilities are implemented such that a sequence of refueling positions or a range of candidate refueling positions can be prescribed and a simulation can be restarted from any previous cycle with altered primary objective and constraints. Multicycle refueling studies over the expected lifetime of a reactor can also be performed efficiently using reduced two-dimensional core models.

KEYWORDS: stable salt reactor, digital twin, online refueling, REBUS

## 1. INTRODUCTION

Fast spectrum molten salt-fueled reactors (MSRs) are receiving increased attention due to their inherent safety features and ability to burn transuranic (TRU) elements in used nuclear fuels, which helps reduce legacy stocks of TRU while contributing to zero-carbon energy production. One of the innovative molten salt-fueled fast reactor concepts is the waste-burning Stable Salt Reactor (SSR-W) [1,2] being developed by Moltex Energy. The SSR-W is a fast reactor fueled with non-flowing static molten chloride fuel salt, which is made of TRU recovered from used CANDU or PWR fuels and cooled by a separate circulating coolant salt. The molten salt fuel is held in static fuel tubes which are further assembled in fuel assemblies like those of conventional solid-fueled reactors. The use of static fuel salt in SSR-W eliminates the complex engineering challenges related to the pumped fuel salt system and leads to an intrinsically safer, simpler, and cheaper molten salt reactor design [3].

---

[a] Current address: Kyoto Fusioneering Ltd., Tokyo, Japan.

SSR-W is designed without control rods (other than safety rods) to reduce the potential risks and accidents associated with control rods. Reactor operation with no control rod is to be achieved by relying on the large negative reactivity feedback of liquid fuel due to thermal expansion and by allowing fuel and coolant temperature variations during normal operations. To limit the temperature variations within a narrow range, the excess reactivity should be small enough. A small excess reactivity requires frequent refueling, and thus online refueling is proposed for SSR-W. In the proposed online refueling scheme for SSR-W, a single burned fuel assembly is discharged at the end of each fuel cycle and a fresh fuel assembly is reloaded in the same position without shuffling to simplify the refueling operation. The cycle length is allowed to vary from a fraction of a day (occasionally) to weeks, with a targeted average cycle length of about one week. For such a simple fuel management scheme, once the fuel assembly design is fixed, the refueling sequence (order and position of each refueled assembly) plays the vital role of determining the core performance metrics such as peak power, average cycle length, average discharge burnup, and so on.

Feasibility investigation and subsequent design optimization of the refueling strategy for SSR-W require intense computer simulations involving multi-physical phenomena. Variations in neutron flux and power distributions, fuel depletion, reactivity perturbation, and thermal feedback need to be modeled for reliable assessment of the performance of specific refueling strategies. For this purpose, a digital twin (DT) system consisting of two functional modules is being developed. The first module DT-1 performs multicycle fuel cycle analysis for a long-term operation of SSR-W while the second module DT-2 performs transient analysis for each refueling operation. In this paper, the development status of DT-1 is presented.

## 2. DIGITAL TWIN FOR REFUELING STRATEGY SIMULATION

The proposed online refueling strategy for a stable salt reactor (SSR) is to discharge a burned fuel assembly and reload a fresh fuel assembly at the same position in each cycle. As mentioned above, the short-term transient phenomena during assembly discharging and reloading are not considered in DT-1. The fuel discharge and reloading are assumed to be completed immediately. Besides, the external fuel cycle processes such as fresh fuel fabrication, storage, and reprocessing of discharged fuel are not included in the fuel cycle analysis under the assumption that a fresh fuel assembly with specified composition is ready to be loaded into the reactor at the end of each cycle. In the simulation of a long-term steady-state operation of a fast spectrum SSR, constant isotopic cross sections for each type of assembly are used without considering burnup dependency and local thermal feedback due to temperature variation. With these assumptions, the multicycle depletion and refueling process of SSR is simulated by performing multicycle fuel depletion calculations at a constant core total power level and determining a reload assembly position at the end of each cycle.

### 2.1. Overall Computational Procedure of DT-1

The digital twin DT-1 is intended for simulating long-term steady-state operation of SSRs by determining a sequence of refueling assembly positions and predicting the core neutronics performances over multiple fuel cycles. In each fuel cycle, it solves the coupled neutron transport and fuel depletion equations, tracks assembly flux, power, burnup, and fuel compositions, and determines a refueling assembly position based on the estimated peak power, reactivity change, and next cycle length corresponding to each candidate refueling position. Because of the similarities in neutronics characteristics of SSR-W to solid-fuel fast reactors, many of the existing fast reactor analysis tools were adopted in DT-1. As shown in Figure 1, DT-1 is developed as a Python wrapper program over the REBUS [4], DIF3D [5], and PERSENT [6] codes of the Argonne Reactor Computation (ARC) code suite, and two newly developed utility codes Reload and Mk1415. The user input data for DT-1 includes a REBUS depletion model at the beginning of fuel cycle, various constraints on the operating conditions, a fresh fuel composition, a composition used to fill a withdrawn assembly space (i.e., coolant), and options for selecting a reload assembly position.

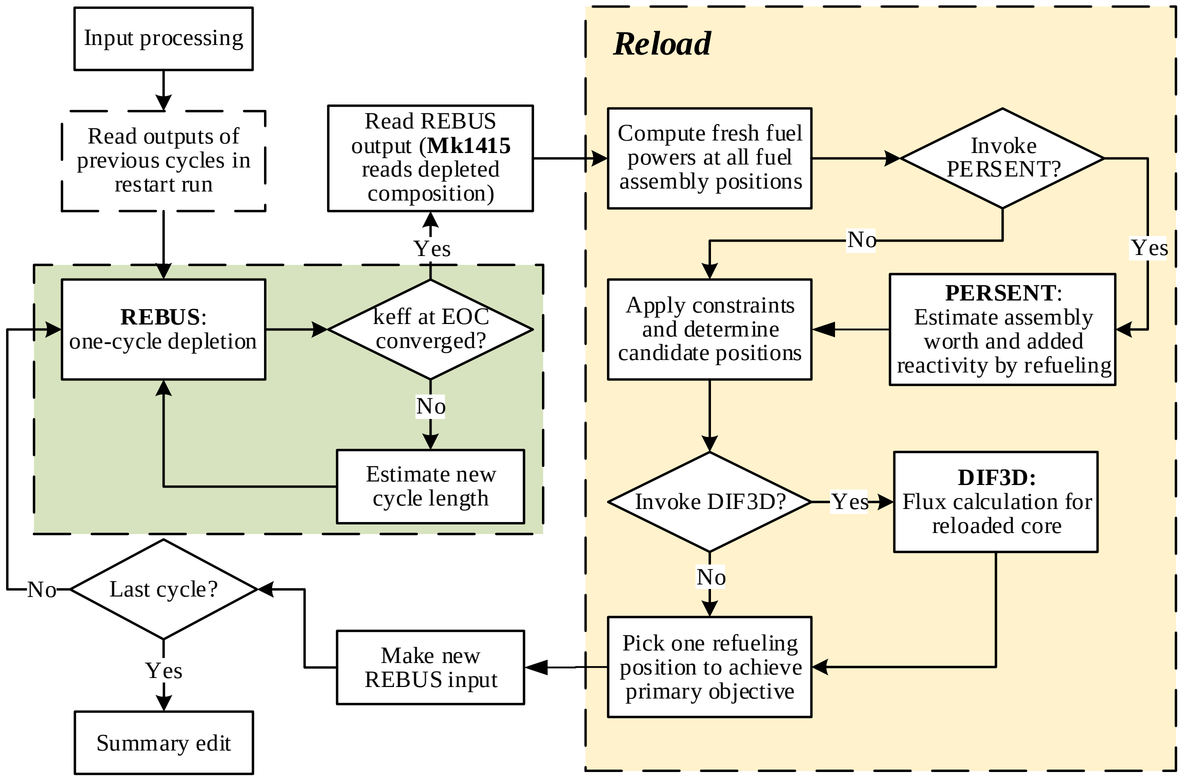


**Figure 1. Overall computational flow of DT-1.**

In a DT-1 simulation, a single fuel cycle analysis with REBUS and a refueling position search with Reload are executed alternately by the Python wrapper. Reload itself is a lower-level wrapper over DIF3D for flux calculations in reloaded core configurations and PERSENT for reactivity calculations. In a REBUS fuel cycle calculation, the cycle length is iteratively determined such that the calculated k-effective value at the end of cycle (EOC) is equal to a user-defined target value within a tolerance limit. After each fuel cycle calculation, a refueling position is selected to achieve a user-specified primary objective while satisfying imposed constraints on operating conditions. Then, a new REBUS input is prepared for the next cycle using the depleted fuel compositions and the user-specified fresh fuel composition. This procedure proceeds repeatedly until the user-specified number of fuel cycles are simulated or terminates when no refueling position satisfies all constraints. DT-1 also has the capabilities to perform a multicycle analysis following a user-prescribed refueling sequence, to confine candidate refueling positions in a specified subset of all the fuel assemblies, or to restart a simulation from any previous cycle. User specifications of the fresh fuel composition, constraints on operating conditions, and primary objective for refueling position search can be changed in a restart run.

## 2.2. Constraints on Refueling Scheme

For safe and economic operation of SSRs, an applicable refueling sequence of fuel assemblies should meet specific constraints on various state parameters. Specifically, in DT-1, the user-specified constraints are applied to the following quantities: (1) maximum assembly power, (2) peak nodal average power density, (3) maximum reactivity worth of fresh fuel assembly, (4) minimum cycle length, (5) minimum discharge burnup, and (6) minimum distance from previous refueling positions.

The peak power limit is applied to the assembly-integrated power as well as the average power density in each axial segment (node) of an assembly, which is an approximate means to limit the allowable assembly-averaged and peak power density in fuel salt. The constraint on the reactivity worth of fresh assembly originates from the nature of online refueling of SSRs as the reloaded fresh fuel assembly should not induce a larger reactivity insertion than what can be accommodated by the negative temperature feedback of liquid fuel salt. Otherwise, the assembly reloading can result in an over-power transient accident. On one hand, the maximum fresh assembly worth also limits the net reactivity addition by replacing a burned assembly with a fresh one and hence determines the achievable cycle length. On the other hand, the allowable minimum cycle length is determined by the physical time required to discharge and reload an assembly. The burnup constraint is applied for economic considerations; a higher discharge burnup is desired to reduce fuel cost including assembly manufacturing. For long-term operation of SSRs, it is necessary to monitor the peak fast neutron fluence of assembly structure. Currently, the peak fast fluence of each discharged assembly is estimated in DT-1 but has not been applied as a rigid constraint when selecting a refueling position.

Other than the above physical constraints, the user can specify to allow or disallow repeated refueling at the same assembly location before all other assembly positions are refueled. DT-1 also allows the user to restrict the minimum distance of the current refueling position from those assemblies recently refueled in the previous fuel cycles to avoid clustered refueling. In the current implementation, DT-1 only performs refueling simulations for a given fresh fuel composition. For a given set of constraints and primary objective, the resulting refueling sequence is a strong function of fresh fuel composition. Depending on the chemical form of fuel salt, the fissile enrichment or the heavy nuclide concentration could be restricted in a range, in which the fuel salt is chemically stable. It is the user’s responsibility to ensure that the specified fresh fuel does exist.

### 2.3. Calculation of State Parameters

DT-1 leverages the legacy ARC codes for neutronics calculations, in which assembly-homogenized core models are used. Specifically, flux solutions are obtained with the variational nodal transport option of DIF3D, i.e., the VARIANT solver [5]. After each REBUS depletion calculation, the assembly and nodal powers, burnups, and flux distributions at EOC are directly available from REBUS output. In Reload, the maximum assembly power and node-averaged power density after refueling are estimated by computing the reloaded assembly power using the fresh fuel composition and the EOC flux solution. Therefore, the perturbation in flux shape due to refueling is not considered. This approximation was verified to induce only small errors, typically less than 1%, in power results. It is because refueling a single assembly does not change the flux distribution drastically. Optionally, a more accurate power distribution can be obtained by invoking a DIF3D calculation for each reloaded core configuration if the user specifies so. Either way, the power distribution in the reloaded core is renormalized to maintain the same nominal total power.

The reactivity loss due to discharge of a burned fuel assembly as well as the reactivity addition due to replacement of burned assembly with fresh assembly are estimated from the first order perturbation theory calculations with PERSENT. Both forward and adjoint fluxes are calculated with VARIANT at EOC. In PERSENT, the reactivity loss due to assembly discharge is estimated by replacing the fuel section of a burned assembly with coolant. The net reactivity addition is estimated by replacing the depleted fuel composition of the discharged assembly with the fresh fuel composition. Using these reactivity changes, the reactivity worth of the reloaded fresh fuel assembly is estimated. The achievable cycle length after refueling is estimated from the predicted reactivity addition and reactivity loss rate in the last cycle. Tests with a SSR core showed that the error in the PERSENT predicted reactivity change due to single-assembly reloading is about 1.0 pcm. Likewise, the user can invoke DIF3D to calculate the accurate reactivity changes due to refueling at each candidate assembly position.

### 2.4. Selection of Refueling Position

Initially, all fuel assembly positions are potential candidates for refueling unless a user-specified subset of them is designated as the search range. A unique refueling position is determined through systematic screening and sorting of candidate positions. The screening process starts with applying the peak power constraints and proceeds with the optional constraints on discharge burnup and minimum distance from previous reload positions. The fresh assembly worth and cycle length constraints are applied at the last. The number of candidate refueling positions is reduced after each screening. Typically, multiple candidate positions are left after applying all the specified constraints. Among the candidate positions that meet all the imposed constraints, a unique refueling position is determined to achieve one of the following primary objectives: (1) minimizing the peak assembly power, (2) minimizing the peak node-averaged power density, (3) maximizing the discharge burnup, (4) maximizing the reactivity addition, and (5) minimizing the deviation of assembly power distribution from a user-specified reference distribution. The user-specified primary objective is achieved based on the state parameters estimated in each cycle. In other words, the local optimum position is selected. The first four objectives are straightforward to understand. The last one is an analogical application of the well-known Haling's principle [7] to maintain an optimized asymptotic power distribution by selecting a refueling position $r$ such that

$$\min_{r\in\text{candidates}} \left\{ \frac{1}{\bar{P}} \sqrt{\frac{1}{N} \sum_{j\in\text{core}} (P_{j,r}^{est} - P_j^{ref})^2} \right\}, \tag{1}$$

where $\bar{P}$ is the core-averaged assembly power, $N$ is the number of fuel assemblies, $P_{j,r}^{est}$ is the estimated power of fuel assembly $j$ when the assembly $r$ is refueled, and $P_j^{ref}$ is the power of assembly $j$ in the reference condition.

In the reload position search, many comparisons of core performance parameters are made to screen out the reload positions violating certain constraints and to identify the position that optimizes a specific primary objective. To eliminate the sensitivity in floating point number comparisons, tolerances are set for different quantities. Different real numbers within the tolerance limit are considered equal. The relative tolerance is set to 0.1% for power and burnup quantities, 0.01% for relative power changes, and 1% for assembly distance. An absolute tolerance of 0.00001 (1 pcm) is used for k-effective and reactivity comparisons. When multiple candidates yield the same primary objective within a tolerance limit, additional performance metrics are considered to determine a unique reload position. The general principle is to choose the candidate having a lower peak power, a higher reactivity addition, and a higher discharge burnup.

## 3. TEST PROBLEM

To demonstrate the refueling simulation capabilities of DT-1, a stable salt reactor test problem (SSRT) was developed based on the Moltex Stable Salt Reactor Waste-burner (SSR-W) concept [2] using open literature information [8] and further simplifications. The planar core configuration of SSRT is shown in Figure 2. SSRT is a molten chloride salt fast reactor fueled with a mixture of solvent salt and trichloride salts of depleted uranium (DU) and recovered TRU from CANDU spent fuels. The core is divided into two regions: inner core (IC) and outer core (OC). An optimum enrichment (i.e., TRU fraction) split between IC and OC was determined to flatten the radial power distribution. For neutronics calculations, an ISOTXS cross section dataset was generated in a 33-group structure using the OpenMC Monte Carlo code [9] based on the ENDF/B-VIII.0 nuclear data library. To simplify the problem, the axial distribution of nuclide densities in the active core due to temperature variation was neglected. Since the fuel salt in each fuel tube is mixed because of natural circulation, each fuel assembly was treated as a single depletion zone in the REBUS model.

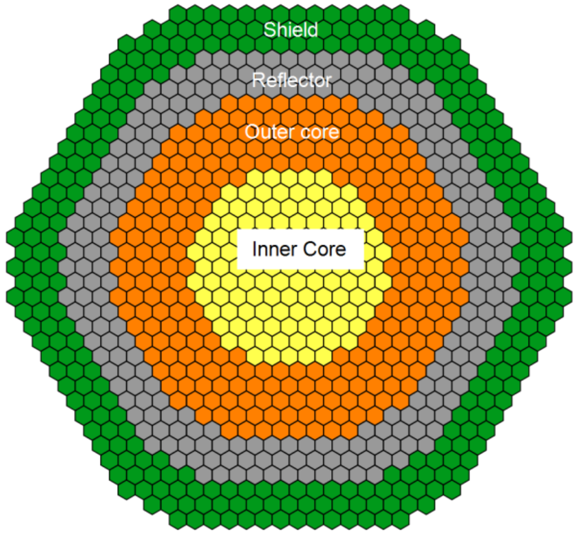


**Figure 2. Core layout of SSRT used for test calculations.**

In refueling simulations, DIF3D flux calculations were performed with the VARIANT $P_1$ diffusion option to save computational time. Specifically, for this problem, the diffusion approximation itself caused less than 200 pcm error in eigenvalue. The impact of this systematic bias on the predicted refueling sequence is a second order effect and is out of the scope of this work. For refueling position search, the following constraints were applied if not specified otherwise. The peak power limit was set to 100 W/cm$^3$ for the assembly-averaged power density in fuel salt. The peak node-averaged fuel power density was limited to 160 W/cm$^3$. Using the core configuration at the beginning of life (BOL), the effective delayed neutron fraction was estimated to be 0.00290 with PERSENT. To avoid an over-power transient accident, the maximum fresh assembly reactivity worth was limited to 200 pcm with a considerable margin to 1$. A minimum cycle length of 1.0 day was allowed with 10% tolerance. The targeted k-effective at EOC of each cycle was set to 1.002, including a 200 pcm margin to criticality to accommodate uncertainties in calculation results. A fuel assembly was allowed to be refueled repeatedly without refueling all other assemblies.

## 4. NUMERICAL RESULTS

Refueling simulations were first performed with a three-dimensional (3D) whole-core model of SSRT. Then, a two-dimensional (2D) model of SSRT was used for long-term simulations. A fresh fuel composition was selected to have 3% less DU than the OC fuel.

### 4.1. Refueling Simulation with 3D Core Model

Table 1 shows the variation of the peak assembly-averaged power density in fuel salt in the first 10 refueling operations determined with the primary objective of minimizing the peak assembly power after each refueling. Here the peak power density refers to the maximum assembly-averaged power density in fuel salt. The ring and position numbers of a refueled assembly are the hexagonal ring and position numbers of DIF3D to represent each assembly position in the hexagonal geometry core. The hexagonal ring number starts from the central assembly and increases outward. In each hexagonal ring, the position number starts from the three o'clock position and increases counterclockwise. This simulation took about 5.6 hours on a Dell PowerEdge R730XD workstation with Intel Xeon E5-2620 processors. In each cycle, the time for refueling position search is more than that for depletion calculation, and the PERSENT calculation to estimate reactivity change is the most time-consuming part.

**Table I. Refueling performance of SSRT with primary objective of minimizing peak assembly power in each cycle**.

| Refueling operation | Cycle length (day) | K-effective | | Peak power density ($W/cm^3$) | | Refueled assembly position | |
|---|---|---|---|---|---|---|---|
| | | BOC | EOC | BOC | EOC | Ring # | Position # |
| 1 | 2.8 | 1.00217 | 1.00201 | 81.22 | 81.21 | 8 | 1 |
| 2 | 3.0 | 1.00217 | 1.00200 | 81.22 | 81.22 | 8 | 8 |
| 3 | 2.9 | 1.00216 | 1.00200 | 81.23 | 81.22 | 8 | 15 |
| 4 | 2.9 | 1.00216 | 1.00200 | 81.12 | 81.12 | 8 | 22 |
| 5 | 2.9 | 1.00216 | 1.00200 | 81.02 | 81.01 | 8 | 29 |
| 6 | 2.9 | 1.00217 | 1.00200 | 80.88 | 80.88 | 8 | 36 |
| 7 | 2.3 | 1.00213 | 1.00200 | 81.04 | 81.04 | 9 | 1 |
| 8 | 2.6 | 1.00215 | 1.00200 | 81.24 | 81.23 | 9 | 2 |
| 9 | 2.9 | 1.00216 | 1.00200 | 81.43 | 81.43 | 9 | 3 |
| 10 | 3.0 | 1.00217 | 1.00200 | 81.61 | 81.60 | 9 | 4 |

### 4.2. Refueling Simulation with 2D Core Model

The refueling simulation with the 3D core model is not efficient for analyzing many fuel cycles. For efficient simulations of a wide range of refueling strategies, a consistent 2D core model with the assembly averaged fuel composition and maintaining the same average linear power as the 3D model of SSRT was used. The average time cost for each cycle was reduced from more than 30 minutes to about two minutes. Because of the neglect of axial leakage, the 2D model overestimated k-effective by ~5330 pcm at the critical state. Therefore, the refueling simulation with the 2D core model was performed using a target EOC k-effective value of 1.0553. Using the same constraints and primary objective, the 2D simulation produced the same refueling positions as the 3D simulation results given in Table I. The core performances for the first 10 refueling operations predicted with 2D and 3D core models are compared in Table II. The deviation of the 2D k-effective from the 3D result remains constant as expected. The 2D model predicted practically the same cycle lengths as the 3D model. The 2D peak power density is consistently higher than the 3D result by ~0.05 $W/cm^3$ because in the 3D model the axial leakage is higher in higher-power assemblies. This test demonstrated that a 2D core model could be used for practical multicycle refueling strategy study.

**Table II. Comparison of cycle length, reactivity, and peak assembly-averaged fuel power density predicted in refueling simulations with 3D and 2D core models**.

| Refueling operation | Cycle length (day) | | Keff difference (2D - 3D) | | BOC peak power density (W/cc) | |
|---|---|---|---|---|---|---|
| | 3D | 2D | BOC | EOC | 3D | 2D |
| 1 | 2.8 | 2.7 | 0.05329 | 0.05329 | 81.22 | 81.27 |
| 2 | 3.0 | 2.9 | 0.05330 | 0.05330 | 81.22 | 81.27 |
| 3 | 2.9 | 2.9 | 0.05331 | 0.05330 | 81.23 | 81.27 |
| 4 | 2.9 | 2.9 | 0.05331 | 0.05330 | 81.12 | 81.17 |
| 5 | 2.9 | 2.9 | 0.05331 | 0.05330 | 81.02 | 81.07 |
| 6 | 2.9 | 2.9 | 0.05330 | 0.05330 | 80.88 | 80.94 |
| 7 | 2.3 | 2.2 | 0.05330 | 0.05330 | 81.04 | 81.09 |
| 8 | 2.6 | 2.6 | 0.05330 | 0.05330 | 81.24 | 81.28 |
| 9 | 2.9 | 2.8 | 0.05331 | 0.05330 | 81.43 | 81.45 |
| 10 | 3.0 | 3.0 | 0.05331 | 0.05330 | 81.61 | 81.60 |

Using the 2D core models, the impact of different primary objectives on the resulting refueling strategies was investigated. The used reload composition contains 3% less DU than the outer core fuel at BOL and all the constraints remain as specified in Section 3. The resulting core performances over 379 refueling operations are compared in Table III. Here "minimize power shape change" stands for the objective of minimizing assembly power distribution deviation from the BOL distribution, and the cycle length statistics do not count in the first cycle starting from BOL, which has a cycle length of 128 days. The peak fuel power density is the maximum assembly-averaged power density in fuel salt over all the cycles. It is seen that refueling strategies have significant impacts on core performances. Figure 3 further shows the detailed evolution of peak fuel power density with different primary objectives. At the first glance, it is counterintuitive that minimizing the peak assembly power in each cycle resulted in a higher peak power density in the long run. This is because a local optimum to minimize the peak power is not necessarily the global optimum over multiple cycles. A refueling position selected in early cycles to reduce the peak assembly power can turn into a peak power position in later cycles. As shown in Figure 4, several OC assemblies near the inner/outer core interface were first refueled. Later, after the peak power occurred at the refueled assemblies, adjacent assemblies are repeatedly refueled to reduce the power share of the peak power assembly. The IC assemblies were seldom refueled mainly because of the constraint of fresh assembly worth.

**Table III. Comparison of refueling strategies with different primary objectives.**

| Primary objective | Minimize peak assembly power | Maximize discharge burnup | Maximize added reactivity | Minimize power shape change |
|---|---|---|---|---|
| Operation time (day) | 1361.2 | 1690.2 | 2117.5 | 1063.1 |
| Max. cycle length (day) | 16.9 | 17.4 | 18.2 | 5.1 |
| Min. cycle length (day) | 1.0 | 2.1 | 2.2 | 0.9 |
| Avg. cycle length (day) | 3.3 | 4.1 | 5.2 | 2.5 |
| Average discharge burnup (MWD/kg) | 17.6 | 27.1 | 37.1 | 16.2 |
| Peak fuel power density (W/cm$^3$) | 93.2 | 92.4 | 92.8 | 87.2 |

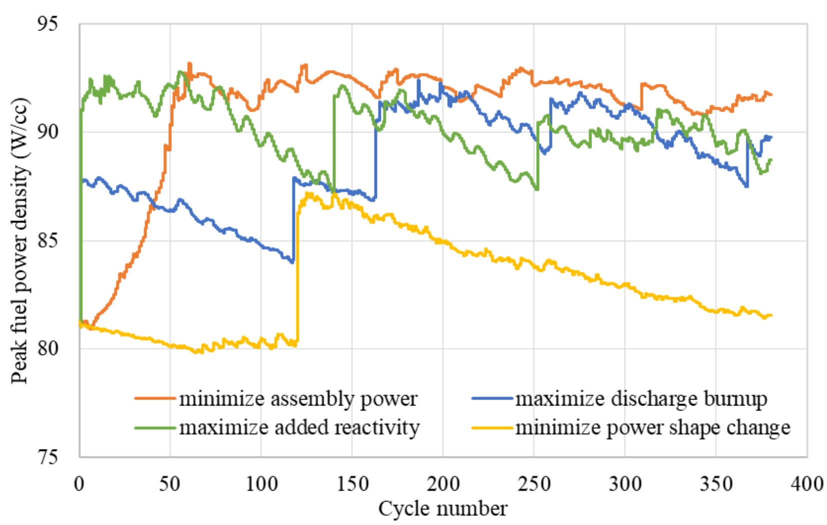


**Figure 3. Evolution of peak assembly-averaged fuel power density with various refueling strategies.**

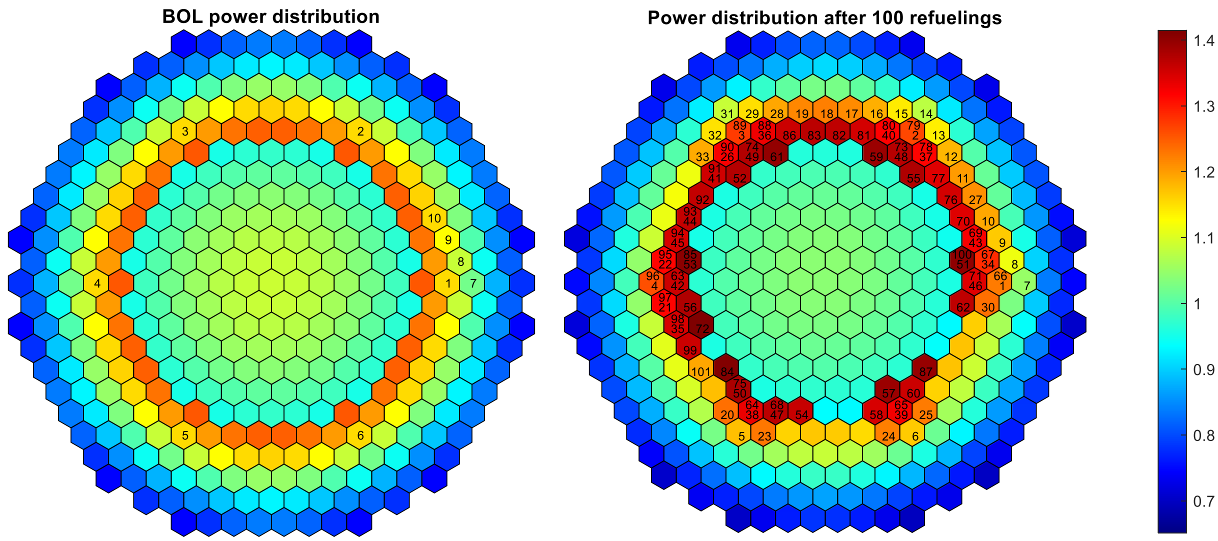


**Figure 4. Relative assembly power distributions and refueling sequences for the primary objective of minimizing peak assembly power. The numbers in hexagon denote the cycles in which the assembly is refueled.**

From Figure 3, the primary objective of minimizing power distribution deviation from BOL seems to yield the flattest power distribution. A further simulation of up to 700 cycles resulted in an evolution history of peak fuel power density and cycle length as depicted in the left plot of Figure 5. It is seen that the peak power density can be well controlled below the imposed power limit and an asymptotic trend is observed. The fluctuation in peak power density is due to the repeated refueling of the outer core. After many cycles, only two periphery IC assemblies were refueled because of the fresh assembly worth constraint, which led to a deeply burned inner core as shown on the right of Figure 5.

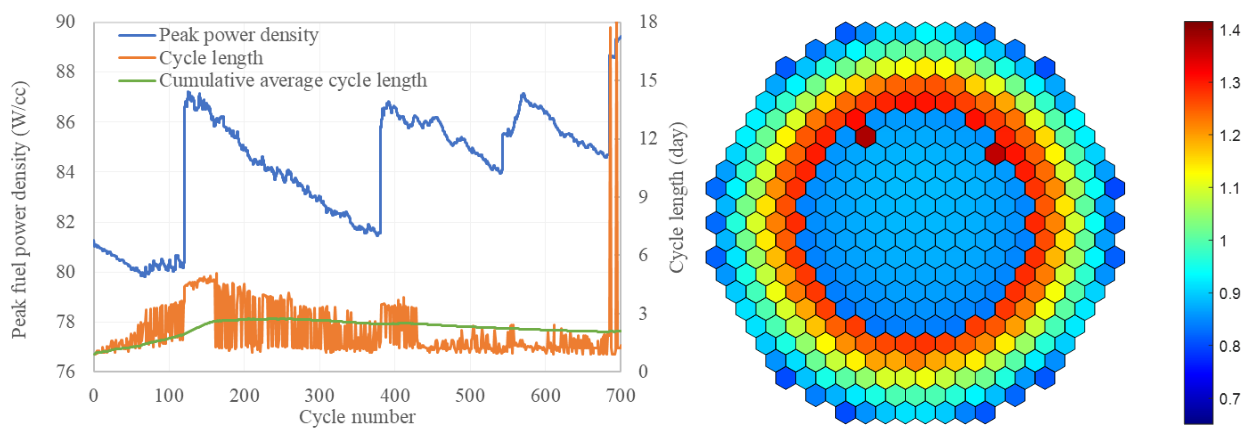


**Figure 5. Left: Evolution of peak assembly-averaged power density in fuel and cycle length for the primary objective of minimizing power distribution deviation from BOL; Right: Relative power distribution after 700 cycles.**

A parametric study confirmed that it is not feasible to refuel the whole core with the selected single fresh fuel composition while satisfying all the imposed constraints. Table IV tabulates the estimated reactivity perturbations and peak assembly-averaged fuel power density corresponding to each refueling at six assembly positions (three IC and three OC assemblies) with three different fuel enrichments. Here the percent changes represent the increase of DU fraction relative to the OC fuel composition at BOL. With fuel burnup, the estimated reactivity worth varies slowly. Nonetheless, depending on the refueling position, certain reload compositions would violate either reactivity worth, peak power, or minimum cycle length constraint.

**Table IV. Estimated peak power and reactivity worth for different reload compositions (varied DU % from initial OC fuel) to refuel six candidate assemblies at BOL.**

| Reload Position | Fresh assembly worth (pcm) | | | Net reactivity addition (pcm) | | | Peak power density in fuel (W/cm$^3$) | | |
|---|---|---|---|---|---|---|---|---|---|
| | +6% | 0% | -6% | +6% | 0% | -6% | +6% | 0% | -6% |
| (1,1) | 188 | 232 | 277 | 43 | 89 | 134 | 82.76 | 95.17 | 107.61 |
| (3,1) | 182 | 224 | 269 | 43 | 86 | 130 | 81.55 | 93.78 | 106.03 |
| (5,1) | 166 | 205 | 245 | 39 | 78 | 118 | 81.23 | 89.37 | 101.03 |
| (7,1) | 137 | 169 | 202 | -32 | 1 | 32 | 81.31 | 81.28 | 91.78 |
| (9,1) | 93 | 116 | 138 | -22 | 1 | 21 | 81.30 | 81.27 | 81.24 |
| (11,1) | 50 | 61 | 72 | -10 | 0 | 10 | 81.29 | 81.27 | 81.25 |

### 4.3. Search for a Whole-Core Refueling Strategy

To find a feasible refueling strategy for long-term operation of SSRT, two fresh fuel compositions were determined for whole-core refueling through a REBUS equilibrium cycle analysis. The SSRT core contains 379 fuel assemblies in total. To mimic the single-assembly refueling strategy, 1/379 of the fuel loading in each assembly is discharged and refueled at the end of each cycle. This procedure is repeated for many cycles and eventually an equilibrium state is achieved by adjusting the refueling compositions for IC and OC to maintain an average cycle length of 7 days. The obtained reload compositions contain about 4% and 5% less DU than the initial IC and OC fuels, respectively. At the equilibrium state, the power distribution is slightly flatter than that at BOL.

Using the searched reload compositions, a refueling strategy was proposed to minimize the assembly power distribution deviation from the power distribution at the beginning of the equilibrium cycle (BOEC). Starting from the outer core, OC and IC assemblies were alternately refueled zone by zone with the capability of confining the candidate refueling positions within each zone. A refueled assembly position is not allowed to be fueled again until all the other assemblies are refueled. All the other constraints remain unchanged from the test problem specification. Figure 6 shows the performance of such a refueling strategy. A total of 1137 refueling operations were simulated and each assembly was refueled three times. The average cycle length and discharge burnup are 4.96 days and 53.4 MWD/kg, respectively. The general trends of peak power density and cycle length approach an equilibrium state. The average cycle length in each of the three sweeps of refueling all assemblies is respectively 4.75, 5.04, and 5.10 days. However, since only a single assembly is refueled each cycle, it is expected that the asymptotic cycle length will still deviate from the equilibrium cycle length achieved by refueling every assembly partially in each cycle.

Through the above test, it is demonstrated that DT-1 can be used to develop a practical refueling strategy for stable salt fast reactors. It is possible to maintain an even flatter power distribution and a longer cycle length with the flexibility to use more reload compositions and to switch refueled zones more frequently. The engineering constraints are the manufacturing cost of different reload compositions and the risk of refueling an assembly with a wrong reload composition.

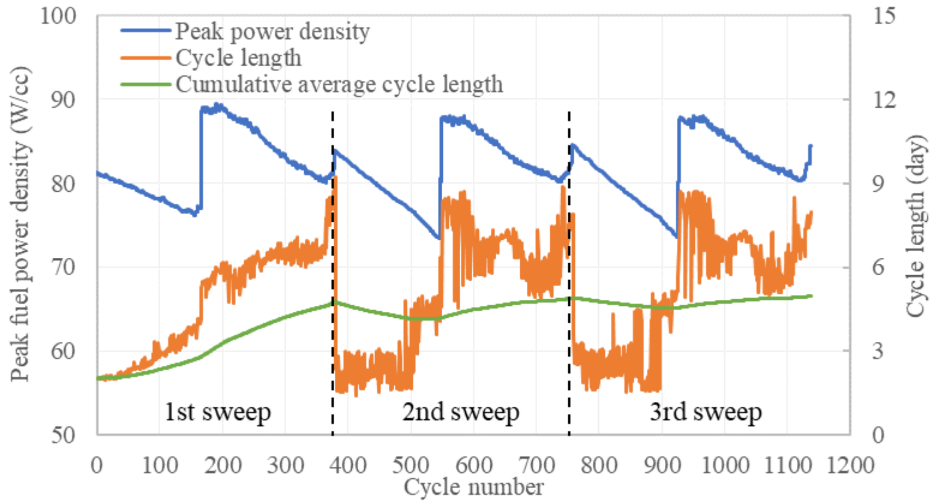


**Figure 6. Evolution of peak assembly-averaged power density in fuel and cycle length with objective of minimizing power distribution deviation from BOEC by refueling OC and IC zone by zone.**

## 5. CONCLUSIONS

To investigate the online fuel management strategy for stable salt reactors (SSRs), a Python wrapped digital twin system DT-1 was developed based on the REBUS, DIF3D, and PERSENT codes. DT-1 provides practical capabilities for simulating the consecutive single-assembly refueling process over many fuel cycles. In each cycle, a refueling position is determined to achieve a user-specified primary objective while satisfying the imposed constraints on the maximum assembly power, maximum node-averaged power density, minimum discharge burnup, maximum reactivity worth of reload assembly, and minimum cycle length. Currently, the primary objective is selected from the following list: (1) minimizing peak assembly-integrated power, (2) minimizing peak node-averaged power density, (3) maximizing reactivity addition, (4) maximizing discharge burnup, and (5) minimizing deviation of assembly power distribution from a user-specified target distribution.

Using a sample SSR core test problem, the DT-1 capability for practical multicycle refueling simulations was demonstrated with the help of 2D core models. Hundreds of refueling operations can be simulated in hours on a small workstation. Test calculations showed that the primary objective for refueling position search has a significant impact on fuel cycle performance. It turned out that minimizing the peak assembly power in each cycle is not an optimum solution to minimizing the peak power in multicycle operation. A feasible refueling strategy was obtained for the sample SSR core by minimizing the deviation of assembly power distribution from a reference distribution obtained in an equilibrium cycle analysis and using different reload fuel compositions for different core regions. However, how to efficiently find the globally optimal multicycle refueling sequence is still an open question, for which a multicycle optimization algorithm needs to be introduced. Optimization algorithms to obtain a global optimum solution over a specified number of cycles are being investigated. Further investigations will also be conducted to enhance efficiency and flexibility further. For example, the capability of adjusting cross section data to reproduce measured state parameters in real operation can be added to accommodate the uncertainties and systematic bias in the computational model.

## ACKNOWLEDGMENTS

This work is supported by UChicago Argonne LLC, Operator of Argonne National Laboratory ("Argonne") under the ARPA-E GEMINA/APPLIED project (Award No DE-AR0001296 led by Moltex Energy). Argonne, a U.S. Department of Energy Office of Science laboratory, is operated under Contract No. DE-AC02-06CH11357. The U.S. government retains for itself, and others acting on its behalf, a paid-up nonexclusive, irrevocable worldwide license in said article to reproduce, prepare derivative works, distribute copies to the public, and perform publicly and display publicly, by or on behalf of the Government. The Department of Energy will provide public access to these results of federally sponsored research in accordance with the DOE Public Access Plan. http://energy.gov/downloads/doepublic-access-plan.

## REFERENCES

1. I. Scott, "Stable salt fast reactor," *Molten Salt Reactors and Thorium Energy*, edited by T. J. Dolan, Woodhead Publishing, Elsevier Science (2017).
2. I. Scott and S. Newton, "The waste-burning Stable Salt Reactor," *Nuclear Engineering International*, March 2022.
3. I. Scott, "Static liquid fuel reactors," *Molten Salt Reactors and Thorium Energy*, edited by T. J. Dolan, Woodhead Publishing, Elsevier Science (2017).
4. W. S. Yang and M. A. Smith, "Theory Manual for the Fuel Cycle Analysis Code REBUS," ANL/NE-19/21, Argonne National Laboratory, 2019.
5. M. A. Smith, E. E. Lewis, and E. R. Shemon, "DIF3D-VARIANT 11.0: A Decade of Updates," ANL/NE-14/1, Argonne National Laboratory, 2014.
6. M. A. Smith, C. Adams, W. S. Yang and E. E. Lewis, "VARI3D & PERSENT: Perturbation and Sensitivity Analysis," ANL/NE-13/8 Rev. 2, Argonne National Laboratory, 2018.
7. R. K. Haling, "Operational Strategy for Maintaining an Optimum Power Distribution Throughout Life," *Proc. Ans. Topl. Mtg. Nuclear Performance Power Reactor Cores*, TID-7672, U.S. Atomic Energy Commission (1964).
8. M. Bushnag, et al., "A Neutronic Study on Safety Characteristics of Fast Spectrum Stable Salt Reactor," *Transactions of the Korean Nuclear Society Autumn Meeting*, Changwon, South Korea, October 20-22, 2021.
9. P. K. Romano, et al., "OpenMC: A State-of-the-Art Monte Carlo Code for Research and Development," *Ann. Nucl. Energy*, **82**, 90–97 (2015).